of the $E^+(L_1)$ level. These equations can be rewritten as

$$4\sqrt{3}\,|\gamma_{1,4}+\gamma_{2,6}| = \pm\{[2E^+(L_1)-A(L_1)-B(L_1)]^2 - [A(L_1)-B(L_1)]^2\}^{1/2}, \quad \text{(C7)}$$

in which

$$A(L_1)=\gamma_{0,1}-6\gamma_{1,1}-6\gamma_{2,1} \quad \text{(C8)}$$

and

$$B(L_1)=\gamma_{0,2}-2\gamma_{1,2}-4\gamma_{1,3}-6\gamma_{2,2}-4\gamma_{2,3}. \quad \text{(C9)}$$

The reality requirement for $(\gamma_{1,4}+\gamma_{2,6})$ leads to the restriction

$$[2E^+(L_1)-A(L_1)-B(L_1)]^2-[A(L_1)-B(L_1)]^2 = \beta_1{}^2-(\alpha_1+36\gamma_{2,2})^2>0. \quad \text{(C10)}$$

The unknowns $\gamma_{2,1}$ and $\gamma_{2,3}$ are eliminated from these equations by use of Eqs. (34), (40)–(42) to obtain

$$\alpha_1=\gamma_{0,1}-(15/2)\gamma_{1,1}-(27/2)\gamma_{1,2}+6\gamma_{1,3} +4[(\gamma_{1,3})^2/\gamma_{1,2}]+3L(\Gamma_{25'})+8M(\Gamma_{25'})+2Q(\Gamma_{25'}) +3[\partial^2E(\Gamma_{2'})/\partial(ak)^2], \quad \text{(C11)}$$

$$A(L_1)+B(L_1)=\alpha_1+18\gamma_{1,2}-12\gamma_{1,3}-2[(\gamma_{1,3})^2/\gamma_{1,2}] -4M(\Gamma_{25'})-4Q(\Gamma_{25'}), \quad \text{(C12)}$$

and

$$\beta_1=2E^+(L_1)-[A(L_1)+B(L_1)]. \quad \text{(C13)}$$

The range of allowed values of $\gamma_{2,2}$ is established by taking the most restrictive of the upper and lower bounds imposed by Eqs. (C4) and (C10).

With an arbitrary value for $\gamma_{2,2}$ but within the range of allowed values, the other six band parameters are evaluated according to the relations

$$\gamma_{2,1}=\tfrac{1}{4}\gamma_{1,1}+\tfrac{3}{4}\gamma_{1,2}-3\gamma_{2,2}-[(\gamma_{1,3})^2/2\gamma_{1,2}]-M(\Gamma_{25'}) -\tfrac{1}{2}L(\Gamma_{25'})-\tfrac{1}{2}[\partial^2E(\Gamma_{2'})/\partial(ak)^2] \quad \text{(C14)}$$

$$\gamma_{2,3}=3\gamma_{2,2}+\tfrac{1}{2}\gamma_{1,3}+[(\gamma_{1,3})^2/4\gamma_{1,2}]-\tfrac{3}{4}\gamma_{1,2}+\tfrac{1}{2}M(\Gamma_{25'}) +\tfrac{1}{2}Q(\Gamma_{25'}), \quad \text{(C15)}$$

$$\gamma_{2,5}=\tfrac{1}{2}\gamma_{1,2}-2\gamma_{2,2}-[(\gamma_{1,3})^2/2\gamma_{1,2}]-M(\Gamma_{25'}), \quad \text{(C16)}$$

$$\gamma_{1,4}=\pm\tfrac{1}{4}[\{\gamma_{0,1}-4\gamma_{1,1}-8\gamma_{2,1}-E^+(X_1)\} \times\{4\gamma_{1,2}-8\gamma_{2,2}+8\gamma_{2,5}-E^+(X_1)\}]^{1/2}, \quad \text{(C17)}$$

$$\gamma_{2,4}=\tfrac{1}{2}\gamma_{1,4}\pm\tfrac{1}{4}[\{L(\Gamma_{25'})-\tfrac{1}{2}\gamma_{1,2}+2\gamma_{2,2}-2\gamma_{2,5}\} \times\{8\gamma_{1,1}-\gamma_{0,1}\}]^{1/2}, \quad \text{(C18)}$$

$$\gamma_{2,6}=-\gamma_{1,4}\pm(1/4\sqrt{3})[\beta_1{}^2-(\alpha_1+36\gamma_{2,2})^2]^{1/2}. \quad \text{(C19)}$$

Arbitrary allowed values of $\gamma_{2,2}$ are scanned and from the resulting energy bands, this parameter is evaluated to obtain the experimental value for the longitudinal cyclotron effective mass.[14,15] In general, several such solutions are found and all mathematically valid solutions are examined. Some of these solutions are, in fact, equivalent and involve only the change in sign of a few band parameters. The most convergent solution also seems to yield the best dielectric constant, and for these two reasons is considered to be the most physical. This solution remains the most convergent under small changes in the band ordering. If, however, a major reordering of the energy bands is made, some other solution might become the most convergent and, therefore, provide the best description of the real solid.

PHYSICAL REVIEW VOLUME 160, NUMBER 3 15 AUGUST 1967

Conductance Anomalies due to Space-Charge-Induced Localized States

D. J. BENDANIEL AND C. B. DUKE
General Electric Research and Development Center, Schenectady, New York
(Received 4 November 1966; revised manuscript received 23 March 1967)

Space-charge-induced accumulation regions in semiconductors and semimetals can lead to localized, discretely spaced two-dimensional energy bands for which the existence criteria and the eigenvalue spectrum are derived. The contribution of these states to the conductance of a planar metal-oxide-semimetal (-semiconductor) tunnel junction exhibits structure associated with the critical points in the density of states for motion parallel to the junction. As an example, numerical results are given for Al-oxide-Bi junctions.

I. INTRODUCTION

THE existence of localized, quantized one-electron eigenstates in narrow accumulation or inversion layers at semiconductor surfaces has been conjectured for at least ten years.[1–3] However, only surface transport measurements[4–8] have given evidence for the existence of these states, and the interpretation of those experiments is qualitative, owing to the lack of a microscopic quantum theory of surface transport.[3] Optical

[1] J. R. Schrieffer, *Semiconductor Surface Physics*, edited by R. H. Kingston (University of Pennsylvania Press, Philadelphia, Pennsylvania, 1957), p. 68.
[2] J. F. Dewald, Ann. N. Y. Acad. Sci. **101**, 872 (1963).
[3] R. F. Greene, Surface Sci. **2**. 101 (1964).
[4] P. Handler and S. Eisenhouer, Surface Sci. **2**, 64 (1964).
[5] N. St. J. Murphy, Surface Sci. **2**, 86 (1964).
[6] F. Proix and P. Handler, Surface Sci. **5**, 81 (1966).
[7] F. F. Fang and W. E. Howard, Phys. Rev. Letters **16**, 797 (1966).
[8] A. B. Fowler, F. F. Fang, W. E. Howard, and P. J. Stiles, Phys. Rev. Letters **16**, 901 (1966).

absorption and tunneling measurements in both semimetals and semiconductors offer the potentiality of a more direct observation of localized-state effects. We consider here tunneling effects, primarily in semimetals. Contributions of localized states to the absorption coefficient in semiconductors are considered by one of us elsewhere.[9]

We outline in Sec. II the existence criteria for the localized states in a metal-oxide-semimetal junction. In Sec. III we calculate the details of their contribution to the conductance. We illustrate, in Sec. IV, our calculations by the example of an aluminum-oxide-bismuth junction. The results of our analysis indicate that contributions from localized states lead to sharp edges and logarithmic peaks in the tunnel conductance for each band. These results are illustrated by sample numerical calculations for (1) a single very narrow band for which all the structure occurs in the neighborhood of zero bias, and (2) a four-band model of bismuth, using perhaps more realistic bandwidths, in which the structure near zero bias is contributed by conduction band edges alone. The structures predicted are qualitatively similar to the data reported by Esaki and Stiles,[10,11] especially in case (1). On the other hand, the reproducibility of tunneling data is sufficiently small[12,13] that quantiative interpretations are unwarranted at the present time. In addition, a more precise determination of the band structure of bismuth and the space-charge potential near the junction are also required before detailed comparison of the predictions of the model with experimental data would be meaningful.

II. LOCALIZED STATES

In Fig. 1 is shown a schematic illustration of the space-charge potential $V(r)$ in a narrow accumulation range. Its depth U and range K_D^{-1} must satisfy the inequality

$$(2m_\perp U/\hbar^2)^{1/2}K_D \gtrsim (\tfrac{1}{2}\pi) \tag{2.1}$$

in which $m_\perp$ is the mass associated with motion normal to the surface of a planar junction. We adopt models of the semiconductor or semimetal in which motion normal to the junction is separable from that parallel to the junction.[14] Equation (2.1) leads to the prediction that localized states are uncommon in tunnel junctions since metal-semiconductor contacts result in depletion regions[15] and metal-oxide-semiconductor junctions usually require thick oxide layers, in order to obtain accumulation regions due either to a positively biased field plate[4–8] or immobile surface charge in the oxide.[16] Although accumulation regions occur in metal-insulator-metal junctions, they are commonly too narrow to satisfy the inequality of Eq. (2.1) except in special cases.

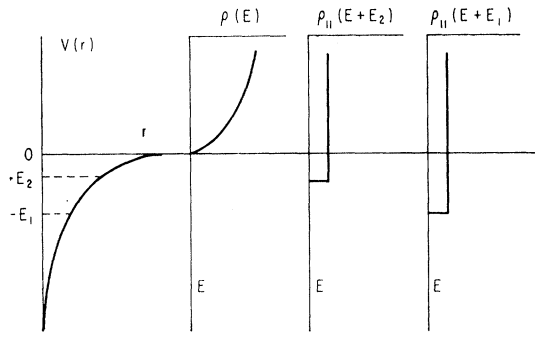

FIG. 1. Schematic illustration of the continuum, $\rho(E)$, and localized-stated band, $\rho_\parallel(E)$, densities of states in a narrow accumulation region associated with a parabolic band.

The satisfaction of Eq. (2.1), hence the occurrence of a localized state, near zero-bias in a tunnel junction requires both a large intrinsic voltage drop across the oxide and a small carrier density on one side of the junction so that a nontrivial portion of the total voltage drop across the junction occurs in this "low-carrier-density" side of the junction. For example, either Bi or Sb constitutes a "low-carrier-density" junction material whose high work function[17] can lead to large electric field in a thin oxide with at least several percent of the total voltage drop occurring in the semimetal. The details of the semiclassical Fermi-Thomas model of the space-charge region have been given earlier.[14] The width of this region is given approximately by

$$L_D = K_D^{-1} = \left[\frac{6\pi n_0 e^2}{\epsilon}\left(\frac{1}{\xi_e}+\frac{1}{\xi_h}\right)\right]^{-1/2} \tag{2.2}$$

in which ϵ is the (static) dielectric constant, n_0 is the (compensated) carrier concentration, and ξ_e, ξ_h are the electron, hole Fermi energies in the semimetal. The details of the potential are easily shown to be

$$\begin{aligned}
&\text{(metal)} && u = -V+\xi_e \quad (x<-x_b)\\
&\text{(oxide)} && u = V_b = -\chi_{OX}+\frac{\varphi_{SM}+\varphi_M}{2}\\
& && \quad -V/2-U/2, \ (-x_b<x<0)\\
&\text{(semimetal)} && u = -Ue^{-K_D x}, \quad (0<x)
\end{aligned} \tag{2.3}$$

where x_b is the oxide thickness, V is the bias applied to the semimetal with respect to the metal, χ_{OX} is the electron affinity of the oxide, φ_M and φ_{SM} are the work

[9] C. B. Duke (to be published).
[10] L. Esaki and P. J. Stiles, Phys. Rev. Letters **14**, 902 (1965).
[11] L. Easki and P. J. Stiles, Phys. Rev. Letters **16**, 574 (1966).
[12] I. Giaever (unpublished).
[13] L. Esaki (unpublished).
[14] D. J. BenDaniel and C. B. Duke, Phys. Rev. **152**, 683 (1966).
[15] See, e.g., D. V. Geppart, A. M. Cowley, and B. V. Dore, J. Appl. Phys. **37**, 2458 (1966).
[16] See, e.g. P. V. Gray, Phys. Rev. **140**, A179 (1965).
[17] *Handbook of Thermionic Properties: Electronic Work Functions and Richardson Constants of Elements*, edited by V. S. Vomenko (Plenum Press, New York, 1966). The several measurements of the work functions do not agree among themselves. This reference seems to be the most accurate and recent compilation of the differing experimental results.

functions of the metal and semimetal, respectively, U is amount of band bending at the oxide-semimetal interface, given by solution of the equation (valid at zero temperature):

$$U=-(\varphi_{SM}-\varphi_M)-V-\frac{x_b\epsilon_{SM}}{\epsilon_{OX}}\left(\frac{16\pi n_0 e^2}{5\epsilon_{SM}}\right)^{1/2}\times D(U)\,\mathrm{sgn}(V), \quad (2.4)$$

where

$$D(U)=\left\{\theta\left(1+\frac{U}{\xi_h}\right)\xi_h\left(1+\frac{U}{\xi_h}\right)^{5/2}-\xi_h+\theta\left(1-\frac{U}{\xi_e}\right)\xi_e\left[1-\frac{U}{\xi_e}\right]^{1/2}-\xi_e\right\}^{1/2}, \quad (2.5a)$$

$$\theta(x)\equiv 1, \quad x\geq 0 \qquad \equiv 0, \quad x<0 \quad (2.5b)$$

In deriving these equations,[14] we assume complete degeneracy, continuity of potential and electric displacement, parabolic electron and hole bands, Fermi-Thomas shielding, and the average, bias-dependent, square barrier specified by Eq. (2.3). The effective mass approximation and a generalized Bethe-Sommerfeld model of the junction are employed throughout our analysis.

The use of (2.1) and (2.2) for the range of the space-charge region, of contact potentials $\sim$0.5 eV,[17] and of thin ($x_b\sim$25 Å) oxides, leads to an expectation of the existence of one or more localized states in the semimetal. One can show that quasistationary states with binding energies $E_{b,i}$ occur at the roots of the equation

$$F_i=-J_p(2Q/K_D)\Big/\left(\frac{m_{OX}Q}{\gamma_i m_{SM,\perp}}\right)J_p'(2Q/K_D)=1, \quad (2.6a)$$

where

$$Q\equiv\left(\frac{2m_{SM,\perp}U}{\hbar^2}\right)^{1/2}, \quad (2.6b)$$

$$\gamma_i\equiv\left[\frac{2m_{OX}}{\hbar^2}(V_b+E_{b,i})\right]^{1/2}, \quad (2.6c)$$

and

$$p\equiv\frac{2}{K_D}\left(\frac{2m_{SM,\perp}E_{b,i}}{\hbar^2}\right)^{1/2}, \quad (2.6d)$$

in which m_{OX} is the mass of electrons in the oxide and $m_{SM,\perp}$ is the mass in the direction perpendicular to the junction in the semimetal. We find that the lifetime τ_i for leakage through the oxide barrier of the ith localized state is given by[18]

$$\tau_i=-\frac{h}{4}\left(\frac{dF_i}{dE}\right)_{E_{b,i}}\frac{\exp(2\gamma_i x_b)}{\sin(2\psi_{Li})}, \quad (2.7a)$$

$$\psi_{Li}=\tan^{-1}\left(\frac{m_M\gamma_i}{m_{OX}k_{\perp,M,i}}\right). \quad (2.7b)$$

The subscript M refers to the metal, x_b is the width of the junction, and $k_{\perp,M,i}$ is obtained by the appropriate kinematics invoking conservation of energy and of the component of momentum parallel to the junction. We recall[18] that the resonance condition, Eq. (2.6a) corresponds to a wave function which lies in the nondegenerate continuum below the bottom of the semimetal conduction band and which is purely decaying in character as one moves through the barrier from the semimetal to the metal. In the limit of a high barrier, $\gamma_i\to\infty$ and Eq. (2.6a) reduces to the eigenvalue condition for bound states in a semi-infinite exponential potential. The inequality of the electron masses and energies of the bottom of conduction band in the metal and semimetal define a one-dimensional barrier-penetration problem for which there is no direct analog in the theory of three-dimensional potential scattering.[19] However, since an appropriately normalized barrier-penetration amplitude is the relevant one-dimensional analog of the collision matrix, it is interesting to observe that complex poles of this amplitude on the second-sheet of the complex energy plane characterize both the energy and lifetime of the one-dimensional localized states in analogy with the conventional description[19] of resonance states in three dimensions. These localized states correspond to quantized bound-states for motion normal to the junction in the potential hole near the junction. The two-dimensional continuum associated with motion parallel to the junction has the consequence that each quantized state causes a two-dimensional energy band of states localized near the junction. The space-charge potential and associated density of states are illustrated schematically in Fig. 1. In semimetals the Fermi energy lies above the band edge in the bulk semimetal so that the two-dimensional energy bands associated with the lowest bulk "electron" band are always partially occupied.

We show in Sec. III that the tunnel conductance contains a contribution proportional to the density of states $\rho_{II}(E)$ of the two-dimensional localized-state bands. Therefore, it is of interest to examine structure in $\rho_{II}(E)$ due to Van Hove singularities above the band minimum. In order to make this examination as illuminating as possible, we consider in detail the case of an s-wave, tight-binding band in a simple tetragonal lattice. The fourfold axis is taken along the z direction and twofold axes along the x and y directions. The Brillouin zone and tight-binding s-band energies for this lattice are illustrated in Fig. 2. The continuum density of states $\rho(E)$ and the density of states $\rho_{yz}(E)$ associated with a localized-state band associated with a junction in the y-z plane are shown in Fig. 3. From Fig. 1 we see that in general the localized-state band is displaced by the binding energy E_i of the quantized state below the local minimum in the band structure out of a superposition of whose continuum states the quantized-state wave func-

[18] E. C. Kemble, *The Fundamental Principles of Quantum Mechanics* (McGraw-Hill Book Company, Inc., New York, 1957), pp. 192–195.

[19] See, e.g. R. G. Newton, J. Math. Phys. 1, 319 (1960).

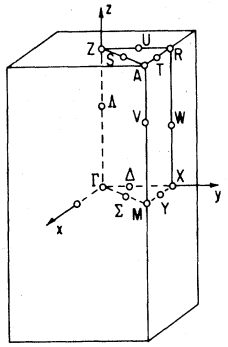

TETRAGONAL BRILLOUIN ZONE

$$E_s(k) = E_1[1-\cos(k_z a_1)] + E_2[2-\cos(k_x a_2)-\cos(k_y a_2)]$$

$$2E_2 > E_1 > E_2$$

FIG. 2. Brillouin zone and tight-binding s-band energies for a simple tetragonal lattice. The a_i are the nearest-neighbor spacings and the energy inequalities have been given for $a_1 < a_2$.

tion is constructed. For the tetragonal s-band, this minimum occurs at the bottom of the band and at $\mathbf{k}=0(\Gamma)$. For a complex covalent material like semimetals local minima occur both above the lowest band minima and at $\mathbf{k}\neq 0$.[20] For example if for a (non-tight-binding) band there is a local minimum at X in Fig. 2, the two-dimensional density of states $\rho_{yz}(E)$ in Fig. 3 could extend from $2E_2$ to the top of the band. In Sec. IV, we in fact construct a four-band model of bismuth in which the "hole" band is described in this manner. More generally, for a local minimum at a given point $\mathbf{P}(\mathbf{k})$ in the Brillouin zone, the two-dimensional density of states extends from $E_L = E(\mathbf{P}) - E_i$ to $E_U = E_L + \Delta E_{11}(\mathbf{P})$ with $\Delta E_{11}(\mathbf{P})$ being the bandwidth for motion in the reciprocal lattice plane, passing through $\mathbf{P}$, which is associated with the plane of the junction. As these two-dimensional bandwidths $\Delta E_{11}(\mathbf{P})$ depend on both the location of the local minimum ($\mathbf{P}$) and the plane of the junction, they can be much smaller than the width of the three-dimensional energy band.

III. CALCULATION OF CONDUCTANCE

We now outline the calculation of the contribution to the current of the localized-state bands in the space-charge region. The general form of the tunnel current, at zero temperature, associated with the continuous electron spectrum for the electron band and barrier illustrated schematically in Fig. 4 is given by

$$J_c = \frac{e}{2\pi^2 h}\int_{\xi_e - eV}^{\xi_e} dE \int_{k_\parallel(0)}^{k_\parallel(E)} d^2k_{11} Z(E,\mathbf{k}_{11}) \quad (3.1a)$$

in which the subscript c denotes the continuum contribution to the current, $Z(E,k_{11})$ is an appropriate barrier penetration factor, and $\mathbf{k}_{11}(E)$ denotes the value of $\mathbf{k}_{11}$ at which the energy of motion parallel to the junction is given by E. The local minimum of the electron bands for a junction normal to the trigonal axis may not have their minima at $\mathbf{k}_{11}=0$, but rather at the symmetry points L at the center of the pseudohexagonal faces of the Brillouin zone.[20] This is the case in bismuth, for example. Recall[14] that $Z(E,\mathbf{k}_{11})$ is calculated keeping E and $\mathbf{k}_{11}$ equal in the initial and final states of the tunneling process. The total energy is related to $\mathbf{k}_{11}$ by

$$E = E_\perp + E_{11}(\mathbf{k}_{11}). \quad (3.2)$$

This fact is often used to convert the integration over d^2k_{11} into one over dE_{11} to give

$$J_c = \frac{2e}{h}\int_{\xi_e - eV}^{\xi_e} dE \int_0^E \rho_{11}(E_{11}) dE_{11} Z(E,E_{11}). \quad (3.1b)$$

In the numerical evaluation of the barrier penetration factor, however, specification of E and $\mathbf{k}_{11}$ in the initial and final states is not sufficient. Strict application of the effective-mass approximation would require conservation of total energy and parallel crystal momentum in the oxide, as well. On the other hand, there is no knowledge of the available eigenstates in the oxide or even its composition. We rely therefore on experimental evidence: If there were no suitable eigenstates in the oxide centered around $\mathbf{k}_{11}(0)$, the displacement of the electron Fermi surfaces of the bismuth, the use of (3.2) in (3.1a) leads to an anomalously small electron barrier penetration. This effect is not observed in the continuum tunneling[12-14] which shows a roughly symmetric dish-shaped conductance. Therefore either such oxide eigenstates apparently exist or $\mathbf{k}_{11}$ conservation must be abandoned. On the other hand, electrons emerging from bismuth into a vacuum, as for example, in field and thermionic emission, also should exhibit this effect. This result would give a marked angular dependence of the work functions.[21] Another possibility, which cannot be

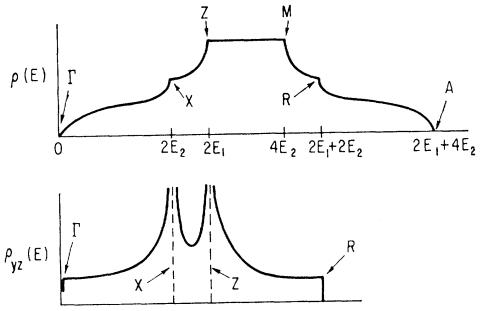

FIG. 3. Continuum density of states, $\rho(E)$, and density of states, $\rho_{yz}(E)$, associated with motion in the ΓZRX plane for a tight-binding s band in a tetragonal lattice. The critical points and energy parameters are defined in Fig. 2.

[20] See, e.g. M. H. Cohen, L. M. Falicov, and S. Golin, IBM J. Res. Develop. 8, 215 (1964).

[21] F. I. Itskovich, Zh. Eksperim. i Teor. Fiz. 50, 1425 (1966); 51, 301 (1966) [English transls.: Soviet Phys.—JETP 23, 945 (1966); 24, 202 (1967)].

ruled out, is the presence of initial-state triplet correlations having the net effect of allowing $\mathbf{k}_{\parallel}(0)=0$ electronic states.

The total current is given by adding to (3.1) the contribution, J_i, due to tunneling into and out of the localized-state bands labeled by i:

$$J=J_c+\sum_i J_i. \tag{3.3}$$

Each band is characterized by a bound-state energy $E_{\perp}=-E_{b,i}$ as shown in Fig. 1 so that E and $E_{\parallel}$ are related by (3.2) and the $dE_{\parallel}$ integration disappears in (3.1). We write

$$J_i=\frac{2e}{h}\int_{\xi_e-eV}^{\xi_e} dE\int_0^E \rho_{\parallel}(E_{\parallel})dE_{\parallel}\frac{\hbar}{\tau(E_{b,i},V)} \times\delta(E-E_{\parallel}+E_{b,i}), \tag{3.4}$$

in which $\tau_i(E_{b,i},V)$ is the lifetime of the localized state, calculated in Sec. II, for leakage through the oxide. Therefore, if tunneling is the rate-limiting factor for the junction current, the current density J_i due to the ith band state is given by

$$J_i=\frac{e}{\pi\tau_i}\int_{\xi_e-V}^{\xi_e} dE\,\rho_{\parallel}(E+E_{b,i}). \tag{3.5}$$

In order to investigate the characteristic structure contributed to the conductance by Eq. (3.5), we consider a model of a two-dimensional band for which $\rho_{\parallel}(E)$ can be evaluated analytically. We choose the simplest prototype of a band with four critical points, the two-dimensional rectangular lattice in the tight-binding approximation, for which $\rho_{\parallel}$ is illustrated in Fig. 3 and is given by[22]

$$\rho_{\parallel}(E+E_{b,i})=(m_{\mathrm{SM},\parallel}/2\pi\hbar^2)\times 0 \quad y\leq 0$$

$$\times\frac{2}{\pi}K(y) \quad (0<y\leq 1) \tag{3.6a}$$

$$\times\frac{2}{\pi}\frac{1}{y}K\left(\frac{1}{y}\right) \quad (y\geq 1)$$

$$y=\left[\frac{(E+E_{b,i})(2[E_1+E_2]-E-E_{b,i})}{4E_1E_2}\right]^{1/2}, \tag{3.6b}$$

in which K is the complete elliptic integral and $2E_1$ and $2E_2$ are the bandwidths in two orthogonal directions parallel to the junction, (see Fig. 2). Equation (3.6) is normalized to give the effective-mass density of states[23] at the lower band edge.

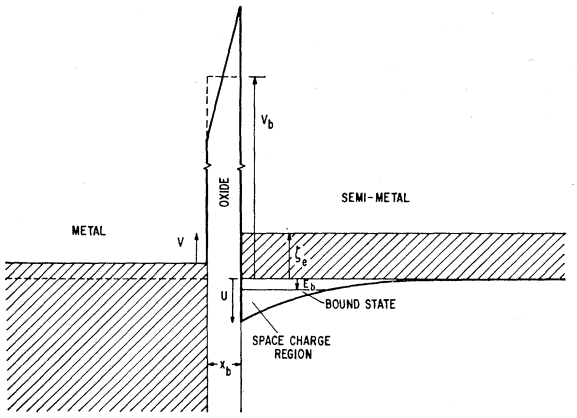

FIG. 4. A schematic diagram illustrating an accumulation region in a metal-oxide-semimetal junction due to the division of the total contact-potential voltage drop between the (thin) oxide and the bulk semimetal.

The contributions to the conductance, $G=(dJ/dV)$, arise from: (a) the ξ_e-eV limit in (3.5) giving a contribution to the conductance proportional to $\rho_{\parallel i}\times(\xi_e-eV-E_{b,i})$, (b) the dependence of E_i on V due to the change in the space-charge potential with bias, and (c) the additional dependence of τ on V because the oxide barrier for $E_{\perp}=-E_{b,i}$ changes with bias.[14] For a fixed barrier, more tightly bound states are associated with longer lifetimes so that part (b) gives rise to a small negative contribution to the conductance which is negligible unless E_i is nearly zero. Part (b) gives a positive contribution for both signs of the bias because a tunneling electron out of (into) the quantized state sees a generally lower barrier in both cases. This contribution gives rise to a positive conductance even when $eV>\xi_e+E_b$ in Fig. 4 because the electrons in the localized-state band tunnel through a barrier which decreases with increasing bias. This conductance due to the bias dependence of the barrier is known to give rise to characteristic effects in metal-semiconductor[24] and p-n junction[14] tunneling as well as in the continuum conductance for metal-oxide-semimetal junctions.[14]

For small bias and deep localized states $E_{b,i}>\xi_e$ the major contribution to the conductance due to each localized state $G_i=dJ_i/dV$ is given by the contribution (a), proportional to $\rho_{\parallel}(\xi_e-eV-E_{b,i})$. Hence the conductivity displays logarithmic Van Hove singularities at $V=E_{b,i}+\xi_e-2E_1$ and $V=E_{b,i}+\xi_e-2E_2$; and abrupt cutoffs at the band edges, $V=E_{b,i}+\xi_e$ and $V=E_{b,i}+\xi_e-2(E_1+E_2)$.[23]

By use of the WKBJ approximation for $Z(E,E_{\parallel})$, one can show further that at zero bias

$$G_i/G_c\sim|E_{b,i}/\xi_e| \tag{3.7}$$

[22] L. Van Hove, Phys. Rev. **89**, 1189 (1953); A. A. Maradudin, E. W. Montroll, and G. H. Weiss, Solid State Phys. Suppl. **3**, 1 (1963).

[23] For the semimetal Bi the mass and Fermi-energy constants are taken from Y. Kao, Phys. Rev. **129**, 1122 (1963); the dielectric constant from C. Nanney, *ibid.* **129**, 109 (1963); and the band widths are estimated from M. H. Cohen, L. M. Falicov, and S. Golin, IBM J. Res. Develop. **8**, 215 (1964). The oxide dielectric constant is an estimate and its surface state density is taken to be zero. The free-electron model is used for the metal. The junction thickness of 25 Å is an estimate based on capacitance measurements due to L. Esaki.

[24] J. W. Conley, C. B. Duke, G. D. Mahan, and J. J. Tiemann, Phys. Rev. **150**, 466 (1966).

so that the contribution to the conductance of a deeply bound localized state is of the same order of magnitude as that of the continuum in a semimetal. The physical interpretation of this result is that a localized-state electron oscillates back and forth inside the space-charge potential thereby having many opportunities to tunnel through the barrier (in the sense of α decay[18]). The continuum electrons, despite their larger number, each get only one opportunity to tunnel. For deeply bound localized states, the greater number of tunneling opportunities outweighs the smaller number of electrons (relative to the continuum) to do the tunneling.

The above comments lead us to the fundamental result of this paper: That for $E_{b,i} \gtrsim \xi_e$ the tunnel conductance contains a contribution proportional to $\rho_{11}(\xi_e - eV - E_{b,i})$ causing logarithmic peaks and sharp edges in the conductance for each band which mirror those shown for $\rho_{yz}(E)$ in Fig. 3, but are shifted from the associated three-dimensional critical points by $E_{b,i}(V)$.

IV. EXAMPLE: BISMUTH-OXIDE-ALUMINUM JUNCTIONS

To provide a quantitative interpretation of experimental conductance data we must know both (a) the parameters of the space-charge region (which are the same for all bands in the effective-mass approximation), and (b) the location $\mathbf{P}(\mathbf{k})$, the energy $E(\mathbf{P})$, and the curvature normal to the junction ($m_\perp$) of all the local minima in the energy-band structure which lie near the Fermi energy. If we anticipate that some of the two-dimensional bands are almost full (i.e., are hole bands) we also must know the bandwidths $\Delta E_{11}(\mathbf{P})$ of the two-dimensional bands associated with a given orientation of the plane of the junction relative to the crystallographic axis, as well as the parameters associated with the locations $\mathbf{P}(\mathbf{k})$ of the *bottom* of such hole bands. These requirements indicate that insufficient experimental data[10–13] exist for a quantiative analysis of the data to be performed at the present time.

We illustrate the qualitative features of the conductance due to localized states, by considering a bismuth-oxide-aluminum junction. As the tunneling experiments in Bi have been made for tunneling normal to the trigonal face,[10] the relevant two-dimensional band structure has threefold rotational symmetry with at least four critical points. Our analysis of Sec. III is thus directly applicable.

The properties of bulk bismuth and band-structure parameters near the electron and hole Fermi surfaces are given by[23] $\xi_e = 17$ meV, $\xi_h = 12$ meV, $\epsilon_{SM} = 100$, $n_0 = 3.5 \times 10^{17}$ cm^{-3}, $\varphi_{SM} = 4.65$ eV, $m_e = 0.05\, m$, and $m_h = 0.15\, m$ using the spherical-band density of states mass for each electron and hole ellipsoid. The oxide parameters are poorly known so we take, somewhat arbitrarily, $m_{OX} = m$, $\epsilon_{OX} = 5-10$, $V_b = 2$ eV, and $x_b = 25$ Å. The free-electron model is used to describe the aluminum with $\xi_e = 11.17$ eV, $\varphi_M = 4.25$ eV, and $m_e = m$ where m is the free-electron mass. In a previous paper,[14] we examined in some detail the dependence of the barrier potential on the oxide parameters and found that a variety of combinations of oxide parameters, metal-semimetal work function differences, and surface-state densities led to the same potential. The best parametrization of the barrier is in terms of the two parameters u and $(du/dV)_{V=0}$ (see Fig. 4 of Ref. 14) and therefore detailed specification of the oxide-parameters and work-function differences is to a large extent superfluous.

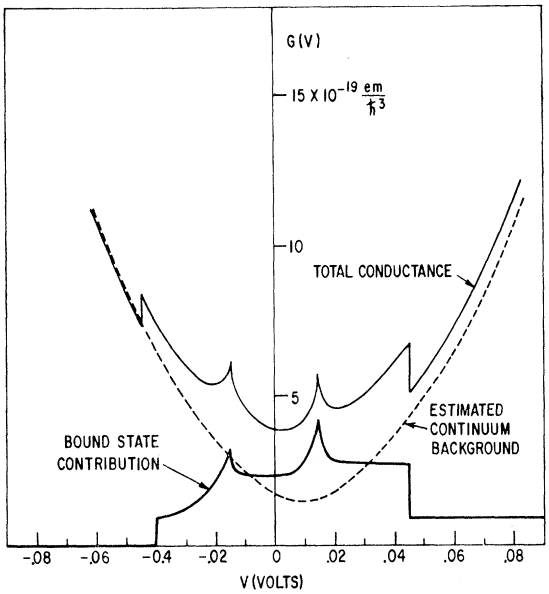

FIG. 5. The tunneling conductance for an aluminum-oxide-bismuth junction obtained using Eqs. (3.5)–(3.7) and the parameters in the text. All the parameters of the bulk materials and junction dimensions were taken from the literature (as specified in Ref. 23) to be relevant to the experiments described in Ref. 10.

Uncertainties in both the electrostatic potential and the band structure of bismuth lead to an enormous variety of possible structures in the conductance. Each localized state solution to Eq. (2.6) for each band leads to a contribution (3.5) to the current in bismuth. Thus for only a single bound state associated with each band [a result which itself depends sensitively on the band structure] one obtains near zero bias, four contributions to the conductance from the four bands in bismuth whose extrema lie close to the Fermi energy.[10,23]

A prototype conductance due to a single, narrow electron band with $E_1 = 7$ meV and $E_2 = 13.5$ meV (giving a bandwidth of 82 meV in a plane normal to the Γ-T line passing through the point L in the Brillouin zone[20]) is shown in Fig. 5. For perspective, it is also shown superposed on the two-band model background due to continuum conductance.[10,14,25] The figure's similarity to

[25] The use of Fig. 2 of a continuum conductance which rises less rapidly away from zero bias would accentuate the effect of the contribution from the localized state. In particular, use of a background conductance extrapolated from Fig. 1 of Ref. 10 would lead to a zero bias conductance maximum of about the same magnitude as shown in that figure.

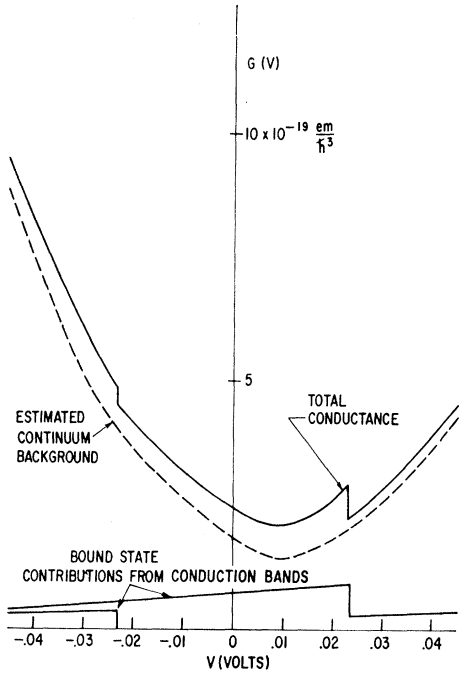

FIG. 6. An illustrative example of the tunneling conductance for an aluminum-oxide-bismuth junction from a four-band model using wider bands with spacings as reported in Ref. 10. A small well depth (~30 MeV) gives rise to a single localized state in each band. The parameters used were the same as those given in the text except that $E_1=0.10$ eV and $E_2=0.11$ eV for all bands, giving band widths of 0.84 eV, and the masses associated with the valence bands were taken as $0.15m$ and $0.5m$, and of the higher lying conduction band as $0.5m$. The contribution of the two valence bands is much smaller than those due to the electron (conduction) bands. The Van Hove singularities due to these bands are well away from zero bias, and only the effect of the band edges is shown.

the data of Esaki and Stiles,[10,11] illustrates the possible role of higher-energy logarithmic similarities in contributing structure to the conductance (although the width of two-dimensional cross section of the band structure used in the calculation giving rise to Fig. 5 appears excessively small and was chosen to display all the structure in the neighborhood of zero bias). For the large localized state, binding energy of 25 meV obtained for Fig. 5 some structure from a higher-lying conduction band will also occur for biases $V\lesssim 10$ meV and $V\geq 55$ meV.

In general, there exist contributions to the conductance from all the bands of the semimetal. For bismuth, four band edges lie within ± 50 meV of the Fermi energy. Taking realistic bandwidths of 840 meV for each band, the contribution of the localized states associated with these bands to the conductance is shown in Fig. 6. Only the conduction bands make observable contributions to this structure, since the tunneling barrier, which is measured from the bottom of the bands, is appreciably higher from the two valence bands, for example, 2 V plus 840 meV for the higher lying valence band.

For thinner junctions, large biases or surface states leading to greater band-bending, more than one trapped state for each band can occur. As a rule of thumb, the number of discretely spaced bands is given by

$$n\approx 2Q/K_D\pi+\tfrac{1}{4}. \tag{4.1}$$

This estimate follows directly from Eqs. (2.6) and therefore is applicable to any exponentially-varying accumulation region.

V. SUMMARY AND CONCLUSIONS

The have shown elsewhere[14] that near a band-edge at E_0 the continuum conductance G_c is proportional to $(eV-E_0)$ in the WKBJ approximation and to $(eV-E_0)^{3/2}$ for a sharp, square-barrier junction. An accumulation region as shown in Fig. 1 alters these results only in the case of a zero-energy resonance for which $G_c\propto(eV-E_0)^{1/2}$. Therefore, in Al-oxide-Bi junctions the conductance due to continuum carriers alone exhibits neither the observed[10] slowly varying zero-bias peak nor the structure superposed on it. If pronounced structure in the tunnel conductance is to be identified with bulk band-structure effects, the mechanism of tunneling via localized states is one effect capable of describing the observed structure. This mechanism also leads to the observed insensitivity of the conductance to the temperature.[10] The large contributions to the current of the localized states is a consequence of specular reflection at the semimetal-oxide interface. The effect of the vastly greater number of continuum electrons in the direction normal to the junction is offset by the fact that each localized electron vibrates back and forth in the accumulation region obtaining many opportunities to tunnel through the barrier. Both the inevitable irregularities in a junction and finite lifetime effects lead to a broadening of the predicted structure.

It is evident that in bismuth, for which four band extrema are thought to lie within ± 50 meV of the Fermi energy, a quantitative interpretation of the conductance data can be attempted profitably only when the location and masses of these extrema have been ascertained independently. If structure occurs in the observed tunnel conductance, it may be caused either by the "surface effect" discussed here; by a junction final-state-interaction (e.g., electron-hole "exciton" correlations across the oxide) or by a variety of "short-circuit" effects in thin oxides.[12] This structure cannot be attributed, in the effective-mass-approximation, to the onset of one-electron tunneling into a new, three-dimensional "continuum" band, however, and any identification of the structure as due to a "bulk" effect directly analogous to those observed in optical absorption must eliminate explicitly the possibility of surface effects.

ACKNOWLEDGMENTS

The authors are indebted to L. Esaki and I. Giaever for discussions of their unpublished data.